

Supporting Information

Microfluidic-integrated laser-controlled microactuators with on-chip microscopy imaging functionality

Jae Hee Jung ^{a, b}, Chao Han ^a, Seung Ah Lee ^a, Jinho Kim ^a, and Changhuei Yang ^a

^aDepartment of Electrical Engineering, California Institute of Technology, 1200 E.

California Blvd., Pasadena, CA, 91125, USA

*^bCenter for Environment, Health, and Welfare Research, Korea Institute of Science and
Technology (KIST), Hwarangno 14-gil 5, Seongbuk-gu, Seoul 136-791, Republic of Korea*

Figure S-1. (a) Focused laser beam spot on a complementary metal–oxide–semiconductor (CMOS) image sensor. (b) Cross-sectional line trace of the horizontal (b1) and vertical (b2) marks of the beam spot. The full width at half maximum (FWHM) of the Gaussian beam profile was $\sim 74\ \mu\text{m}$. (c) Power of the focused laser beam as a function of laser current.

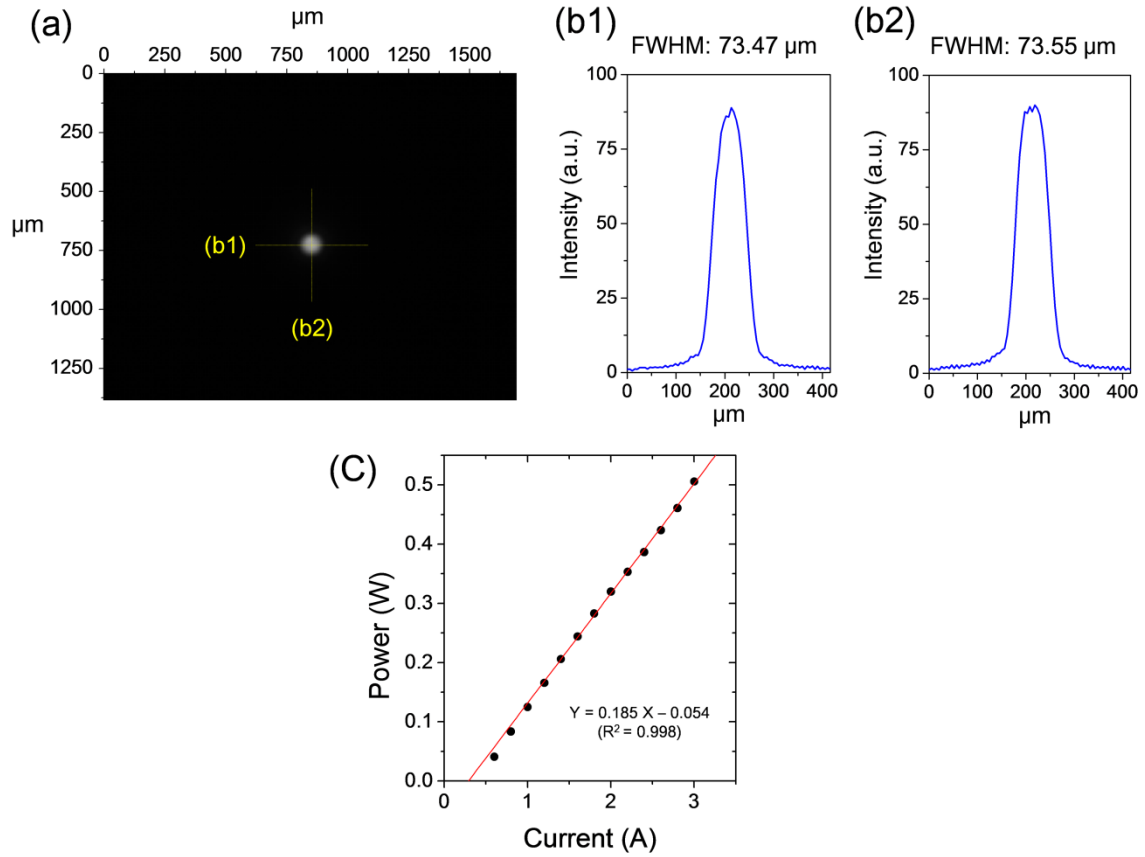


Figure S-2. Fabrication process for the microfluidic component and its attachment to the image sensor. (a) Using standard micromolding processes,^[1] SU-8 photoresist (thickness: 160 μm) was patterned onto a 3-inch silicon wafer to form a master. (b) Liquid PDMS prepolymer solution was poured onto the master and cured at 80°C for 2 h. (c) The PDMS structure was peeled off from the master. (d) The 0.75-mm and 1.2-mm holes were punched to form the inlet of the cell/medium, paraffin wax, and drug/medium. (e) The resulting microfluidic structure was bonded onto the image sensor after oxygen plasma treatment (40 W, 30 s). (f) After injection of paraffin wax and working fluid into the microactuator chamber and material chamber, a thin glass coverslip (CS-8S, Warner Instruments, USA; 8 \times 8 mm, thickness: \sim 0.15 mm) was used as a cover for the integrated microfluidic chip.

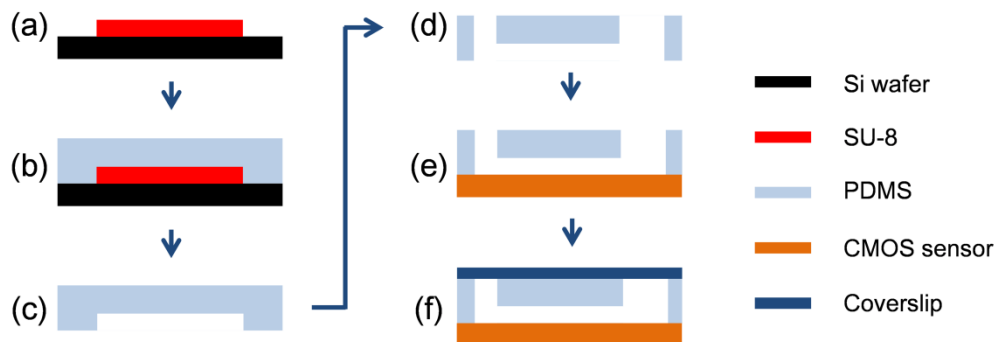


Figure S-3. Sensor surface temperature measurement during imaging of the full field-of-view (FOV) in the cell incubator (37°C). A thermoelectric cooler (TEC) (power input = 7.7 W) was used during imaging to prevent the sensor surface temperature from exceeding 37°C. The TEC was switched on 1 min before imaging for precooling. Five measurements were repeated in total. The 0–130 s is for stand-by, 130–190 s for pre-cooling, and 190–230 s for imaging.

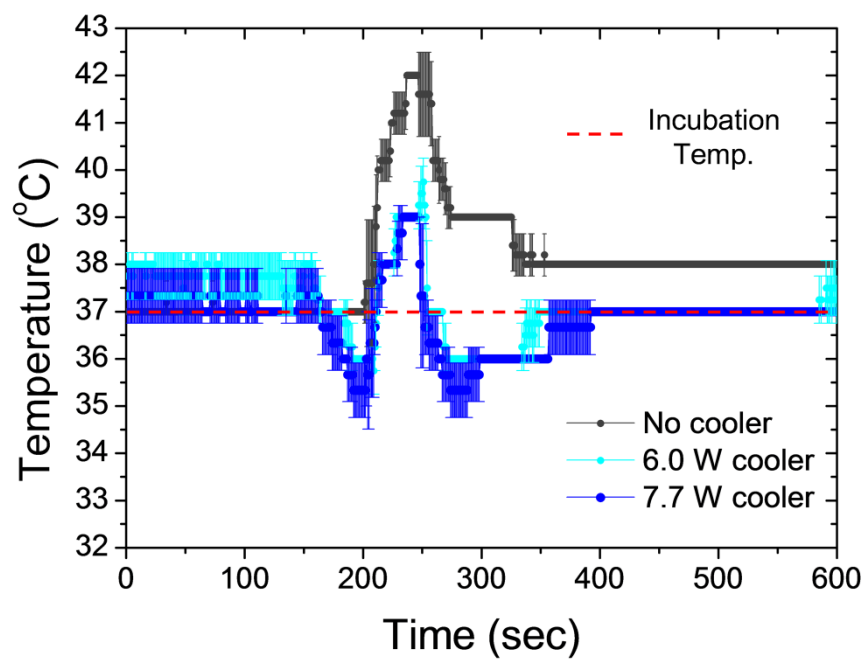
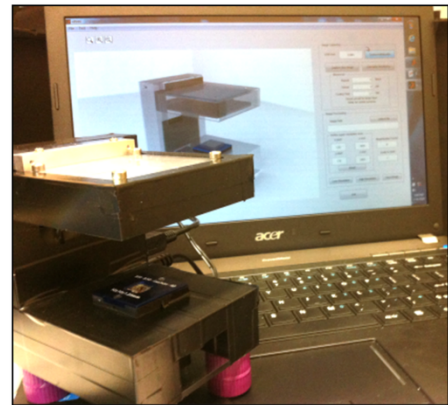
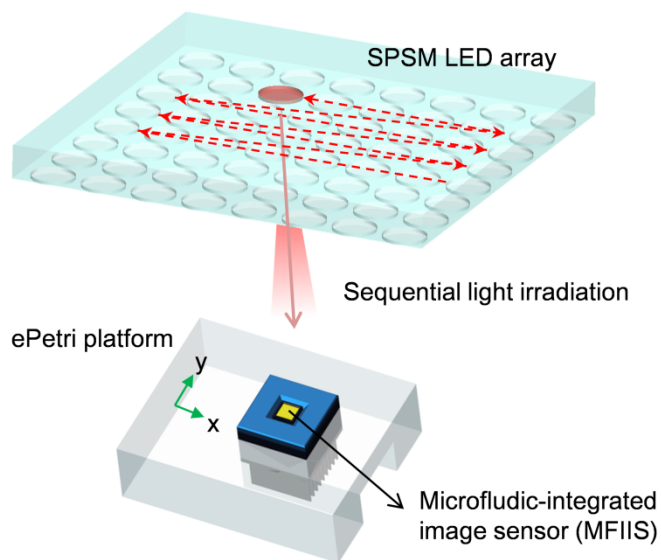
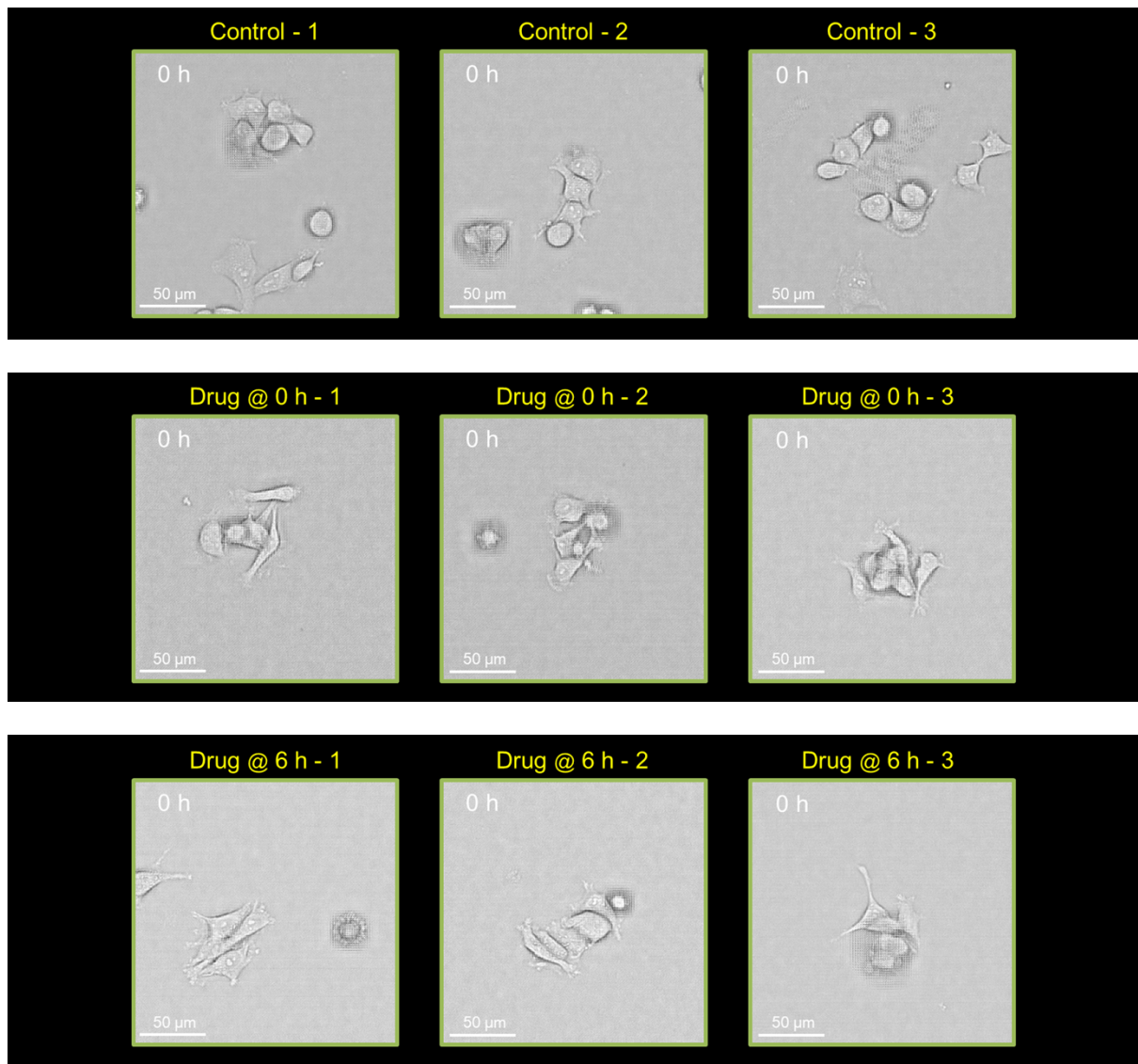


Figure S-4. Schematic diagram of the subpixel sweeping perspective microscopy (SPSM) technique on the ePetri platform. Each LED in the 8×8 LED array is turned on sequentially. As the illumination scans, the image sensor captures the light transmitted through the sample under each LED. The raw images have low-resolution (limited by the pixel size ($2.2 \mu\text{m}$) of the image sensor). Each frame represents a view of the object that is laterally shifted with respect to the next due to the varying angle of incidence in the scanning illumination. The pixel super-resolution reconstruction accounts for the different spatial information in each of the 64 low-resolution images and restores a single high-resolution image. More details of the image acquisition and reconstruction algorithm are described in our previous study.^[2, 3]



Movie S-1. Time-lapse imaging of living cells undergoing camptothecin (CPT) treatment (1 μ M): the control group and the CPT group (i.e., Drug group). Movie S-1 shows the reconstructed high-resolution (HR) time-lapse images of cells from a specific three sub-locations undergoing CPT treatment.



References

- [1] J. R. Anderson, D. T. Chiu, H. Wu, O. J. Schueller, G. M. Whitesides, *Electrophoresis* **2000**, *21*, 27.
- [2] G. Zheng, S. A. Lee, Y. Antebi, M. B. Elowitz, C. Yang, *Proc. Natl. Acad. Sci. USA* **2011**, *108*, 16889.
- [3] S. A. Lee, J. Erath, G. Zheng, X. Ou, P. Willems, D. Eichinger, A. Rodriguez, C. Yang, *PloS one* **2014**, *9*, e89712.